Biochimica et Biophysica Acta 1798 (2010) 1876–1885

Contents lists available at ScienceDirect

Biochimica et Biophysica Acta

journal homepage: www.elsevier.com/locate/bbamem

Interactions of oritavancin, a new semi-synthetic lipoglycopeptide, with lipids extracted from *Staphylococcus aureus*

Oscar Domenech [a], Yves F. Dufrêne [b], Françoise Van Bambeke [a], Paul M. Tukens [a], Marie-Paule Mingeot-Leclercq [a,*]

[a] Université catholique de Louvain, Louvain Drug Research Institute, Unité de pharmacologie cellulaire et moléculaire, UCL 73.70, avenue E. Mounier 73, B-1200 Bruxelles, Belgium
[b] Université catholique de Louvain, Faculté d'ingénierie biologique, agronomique et environnementale, Unité de chimie des interfaces, Place Croix du Sud 2, B-1348 Louvain-la-Neuve, Belgium

ARTICLE INFO

Article history:
Received 5 February 2010
Received in revised form 25 May 2010
Accepted 11 June 2010
Available online 23 June 2010

Keywords:
Vancomycin
Oritavancin
Lipoglycopeptides
Staphylococcus aureus
POPE
POPG
Cardiolipin
lysylDOPG
Lipids
Laurdan
DPH
ANS
Calcein release
AFM

ABSTRACT

Oritavancin, a lipoglycopeptide with marked bactericidal activity against vancomycin-resistant *Staphylococcus aureus* and enterococci, induces calcein release from CL:POPE and POPG:POPE liposomes, an effect enhanced by an increase in POPG:POPE ratio, and decreased when replacing POPG by DPPG (Domenech et al., Biochim Biophys Acta 2009; 1788:1832–40). Using vesicles prepared from lipids extracted from *S. aureus*, we showed that oritavancin induces holes, erosion of the edges, and decrease of the thickness of the supported lipid bilayers (atomic force microscopy; AFM). Oritavancin also induced an increase of membrane permeability (calcein release) on a time- and dose-dependent manner. These effects were probably related to the ability of the drug to bind to lipid bilayers as shown by 8-anilino-1- naphthalene sulfonic acid (ANS) assay. Interaction of oritavancin with phospholipids at the level of their glycerol backbone and hydrophobic domain was studied by monitoring changes of Laurdan excitation generalized polarization (GP_{ex}) and 1,6-diphenyl-1,3,5-hexatriene (DPH) fluorescence anisotropy upon temperature increase. Oritavancin increased GP_{ex} values and the transition temperature, indicating a more ordered structure at the level of the glycerol backbone. Oritavancin slightly decreased DPH fluorescence depolarization intensities, suggesting an increase in fluidity at the level of acyl chains. Together, our data confirm the interaction of oritavancin with lipids and the potential role of a rigidifying effect at the level of glycerol backbone for membrane permeabilization. This work shows how AFM and biophysical methods may help in characterizing drug–membrane interactions, and sheds further light on the mode of action of oritavancin.

1. Introduction

The bacterial envelope fulfils several functions essential for survival such as maintenance of cell shape, resistance to turgor pressure, and coordinated cell growth and division. It also acts as a molecular sieve and plays an important role in molecular recognition and cellular interactions. Because of these functions and of marked differences in composition from the envelope of eukaryotic cells, the bacterial envelope stands as a desirable drug target [1]. Thus, a large number of antibiotics acting on peptidoglycan, such as β-lactams and glycopeptides, have been successfully brought in clinical use since many years. In contrast, and with the exception of nisin (used as food preservative), molecules acting on the membrane part of the bacterial envelope have remained ill developed for many years. This is now changing rapidly, because of the increased resistance manifested by bacteria towards β-lactams, glycocopeptides, and several other classes of antibacterials. Starting from the naturally occurring polymyxins [2] and lipoptaibols [3,4], several investigators have synthesized fatty acid conjugates of various peptides or proteins such as cathepsins G [5], lactoferrin [6,7], magainins [8], or, in the context of antiparasitic chemotherapy, a cecropin-melittin hybrid peptide [9]. Another approach has been to start from existing antibiotics and to construct amphipathic derivatives, such as those made from aminoglycosides [10,11] or glycopeptides [12,13]. Among the latter, telavancin and oritavancin show remarkable bactericidal activity towards Gram-positive bacteria, related, at least in part, to their selective membrane destabilization properties [14,15]. These have now reached an advanced level of clinical development for the treatment of severe infections caused by multiresistant *Staphylococcus aureus* [16].

Oritavancin is of particular interest in this context because it shows activity not only against *S. aureus* resistant to β-lactams (so-called "methicillin-resistant S. aureus" [MRSA]), but also against *Enterococci* and *S. aureus* that have become resistant to vancomycin by modification of the D-Ala-D-Ala motif in nascent peptidoglycan [17], and to which

* Corresponding author. Tel.: +32 2 764 73 74; fax: +32 2 764 73 73.
E-mail address: marie-paule.mingeot@uclouvain.be (M.-P. Mingeot-Leclercq).

0005-2736/$ – see front matter © 2010 Elsevier B.V. All rights reserved.
doi:10.1016/j.bbamem.2010.06.011

vancomycin must bind to exert its antibacterial effects [18,19]. Oritavancin is also active against bacteria in stationary phase, including biofilms [15,20]. This suggests a mode of action largely independent from the biosynthesis of the bacterial envelope, in contrast to β-lactams [21] and vancomycin [22].

Two key structural features distinguishing oritavancin from vancomycin are a chloro-biphenyl methylene side chain and an epivancosamine moiety (see structures in [23]). Together, these confer a marked amphipathic character to the molecule [12]. While the consequences of these changes on the membrane effects caused by oritavancin are not entirely known, recent work has demonstrated the capacity of the drug to disrupt membrane potential and to increase the permeability of liposomes composed of binary mixture of lipids [23]. In this model, oritavancin causes rapid and complete release of calcein from CL:POPE liposomes, and slower but still substantial release from POPG:POPE liposomes. This effect is concentration-dependent, is enhanced by an increase in POPG:POPE ratio, and is decreased when POPG is replaced by DPPG. AFM of CL:POPE supported bilayers also showed that oritavancin causes a remodeling of the lipid domains combined with a redisposition of the drug and degradation of the borders. In all these studies, vancomycin, at the concentrations examined in these studies, was without significant effect [23].

The intrinsic activity and the specificity of drugs that target lipids are, however, related to defined structures and arrangements [24,25], which can be critically dependent upon the global lipid content. It is, therefore, important to characterize the capacity of oritavancin to interact with lipids using models that are as relevant as possible to bacterial membranes. In the present study, supported lipid bilayers and liposomes were prepared from lipids extracted from *S. aureus*. Supported lipid bilayers were used to characterize, by atomic force microscopy, the effect of oritavancin on the nanoscale lipid organization. Using liposomes (large unilamellar vesicles [LUV]), we measured the effect of oritavancin on membrane permeabilization using calcein as a probe and determined the binding of 8-anilino-1-naphthalene sulfonic acid (ANS) on liposomes incubated with oritavancin. We also characterized the effect of oritavancin on the polar head group region and the hydrocarbon core using 6-dodecanoyl-2-dimethylaminonaphthamene (Laurdan) and , 6-diphenyl-1,3,5-hexatriene (DPH), respectively. Finally, to further explore the specific role of the main lipids found in membranes of *S. aureus*, we investigated these two last parameters on liposomes composed of synthetic lipids (LysylDOPG:POPG:POPE and CL:POPE). Vancomycin was used as a comparator in all these studies.

2. Materials and methods

2.1. Materials

The ATCC25923 *S. aureus* strain (laboratory standard; fully susceptible to both β-lactams [MSSA] and vancomycin) was used in this study. Beef heart cardiolipin (CL; disodium salt; purity>99%), 1-palmitoyl-2-oleoyl-*sn*-glycero-3-phosphoglycerol (POPG), 1,2-dioleoyl-*sn*-glycero-3-[phospho-*rac*-(3-lysyl-(1-glycerol))], HCl (Lysyl-DOPG), and 1-palmitoyl-2-oleoyl-*sn*-glycero-3-phosphoethanolamine (POPE) were purchased from Avanti Polar Lipids (Alabaster, AL) and used without further purification. Calcein was purchased from Sigma-Aldrich (St. Louis, MO) and was purified as described previously [26]. Briefly, calcein was dissolved in 6 N NaOH and subjected to size-exclusion chromatography through a Sephadex® LH-20 column. The final concentration of calcein solution in 20 mM Tris–HCl was 73 mM with an osmolality of 434 mOsm/kg (measured by the freezing point technique, using a model 3C2 Advanced Cryomatic Osmometer [Advanced Instruments, Needham Heights, MA]). ANS (8-anilino-1- naphthalene sulfonic acid), DPH (1,6-diphenyl-1,3,5-hexatriene), and Laurdan (6-dodecanoyl-2-dimethyl-aminonaphthalene) were purchased from Molecular Probes (Invitrogen, Carlsbad, CA) and used without further purification. Oritavancin diphosphate powder was supplied by Targanta Therapeutics (Cambridge, MA; presently The Medicines Company, Parsippany, NJ), as microbiological standard for *in vitro* investigations. It was dissolved in water containing 0.002% polysorbate-80 (vol:vol), according to the manufacturer's instructions and the recommendations of the Clinical and Laboratory Standard Institute [27], to prevent adhesion to plastic surfaces [28]. For this reason, all effects of oritavancin were studied, and are presented in comparison with liposomes exposed to 0.002% polysorbate-80 alone. Vancomycin was obtained from GlaxoSmithKline s.a. (Genval, Belgium) as the product registered for parenteral use in humans and complying with the provisions of the European Pharmacopeia (vancomycin–HCl; no excipient). The minimal concentrations of oritavancin and vancomycin that inhibit the growth of vancomycin-susceptible *S. aureus* (MIC) are typically around 0.04 and 0.69 μM (0.064 and 1 mg/L), respectively, and the concentrations at which bactericidal effects are observed (minimal bactericidal concentrations [MBC; 3 $\log_{10}$ decrease in colony forming units [cfus]) are around 0.11 μM and 5.5 μM (0.2 and 8 mg/L) [29,30].

2.2. Extraction of lipids from S. aureus

Lipids were extracted using a modified Bligh and Dyer method to prevent the degradation of lysylphosphatidylglycerol into phosphatidylglycerol. Briefly, bacteria were grown in Mueller Hinton Broth until exponential phase (OD = 0.6, λ = 620 nm). They were collected by centrifugation at 3,000×*g* for 15 min and washed three times by resuspending the pellet in 10 mM Tris–HCl, pH 3.0. Extraction steps included: (a) the addition of 1.5 mL of $CHCl_3$-CH_3OH (2:1, v/v) to 0.4 mL of the bacterial suspension and vigorous vortexing for 5 min; (b) the addition of 0.5 mL of $CHCl_3$ and 5 min vortexing; (c) the addition of 0.5 mL of 10 mM Tris–HCl, pH 3.0 and 5 min vortexing; (d) a centrifugation (1000×*g*, 5 min) to allow separation between the organic and aqueous phases. The organic phase was collected and dried, and the extracted lipids were resuspended in $CHCl_3$-CH_3OH (2:1, v/v) and stored at −20 °C in a N_2 atmosphere.

2.3. Large unilamellar vesicles preparation

The solvent ($CHCl_3$:CH_3OH [2:1, v/v]) in which lipids (extracted or synthetic) were dissolved, was evaporated using a Rotavapor system (model R-210, Buchi Labortechnik AG, Flawil, Switzwerland). Dried films were maintained under reduced pressure overnight and thereafter hydrated with 20 mM Tris–HCl, 150 mM NaCl, 20 mM $CaCl_2$ pH 7.4 for AFM studies, with the purified calcein for permeability experiments and with 10 mM Tris–HCl, pH 7.4 for the experiments with ANS, DPH and Laurdan. Large Unilamellar Vesicles (LUV) were obtained after 5 cycles of freeze/thawing and 10 cycles of extrusion in a 10 mL Thermobarrel Extruder (Lipex Biomembranes, Vancouver, Canada) under a nitrogen pressure of 10 bars through two polycarbonate filters of 100 nm or 400 nm pore size for fluorescence studies and AFM studies, respectively (Nucleopore, Costar Corporation, Badhoevedorp, The Netherlands). Non-entrapped calcein was removed using minicolumn centrifugation. As reported in literature, large unilamellar vesicles with diameter>40 nm exhibit an equal distribution of lipid across the membrane. The size and polydispersity of liposome suspensions were monitored by quasi-elastic light scattering with a Zetasizer Nano SZ (Malvern Instruments, Worcestershire, UK). Lipid concentration on the liposomal suspensions was measured by phosphorous quantification as previously described [31].

2.4. Atomic force microscopy

Before each experiment, the contact mode cell was extensively washed with ethanol and water. Mica squares (0.25 cm^2) were glued onto a steel disc, cleaned carefully with water before use and cleaved

to obtain a flat and uniform surface. Immediately, an aliquot of 50 μL of vesicles (*S. aureus* lipid extraction in 20 mM Tris–HCl, 150 mM NaCl, 20 mM $CaCl_2$, pH 7.4), was deposited on the mica surface and incubated for 1 h at room temperature. This method involved liposome fusion which did not allow to control the lipid asymmetry. The sample was thereafter washed with buffer (20 mM Tris–HCl, 150 mM NaCl, pH 7.4) to eliminate non-adsorbed vesicles. AFM contact mode images in liquid were obtained using a Nanoscope IV Multimode AFM (Veeco Metrology Group, Santa Barbara, CA) with triangular Si3N4 cantilevers (Microlevers, Veeco Metrology Group, Santa Barbara, CA.) with a nominal spring constant of 0.01 $N \times m^{-1}$. The instrument was equipped with a "J" scanner (120 μm). To minimize the applied force on the sample the set point was continuously adjusted during imaging. Images were acquired at 90º scan angle with a scan rate of 2 Hz. All images were processed using the Veeco software.

2.5. Permeability studies

Membrane permeabilization was followed by monitoring the leakage of entrapped, self-quenched calcein from liposomes upon measuring the increase of fluorescence signal subsequent to its dilution in the external medium [32]. The liposome total phospholipid concentration was adjusted to a final concentration of 5 μM with isoosmotic buffer (20 mM Tris–HCl, 200 mM NaCl, pH 7.4). After overnight storage at 4 °C, liposomes were exposed to the drug under study at 37 °C at the desired concentration and for the suitable time with continuous stirring and protection from light. All fluorescence determinations were performed on an LS 55 fluorescence spectrophotometer (Perkin-Elmer Ltd., Beaconsfield, UK) using λ_{exc} and λ_{em} of 476 nm and 512 nm, respectively, and slits fixed at 3 nm. The percentage of calcein released under the influence of drug was defined as $[(F_t\text{-}F_{contr})/(F_{tot}\text{-}F_{contr})]\times 100$, where F_t is the fluorescence signal measured at time t in the presence of drug, F_{contr} is the fluorescence signal measured at the same time in the absence of drug, and F_{tot} is the total fluorescence signal obtained after complete disruption of liposomes by Triton X-100 at a final concentration of 2% (checked by quasi-elastic light spectroscopy).

2.6. Binding experiments

Drug interactions with lipids were assessed using a fluorescence-based assay using ANS. This negatively charged, fluorescent probe has a low fluorescence yield in polar environments, which is greatly enhanced when it interacts with lipids. ANS was dissolved at final concentration of 5 mM in methanol. The liposome total phospholipid concentration was adjusted to a final concentration of 50 μM with 10 mM Tris–HCl pH 7.4. The experiments consisted of incubating liposomes with the drugs (60 nM) for 60 min at 37 °C. The samples were then titrated with ANS and fluorescence was monitored. All fluorescence determinations were performed on an LS 55 fluorescence spectrophotometer (Perkin-Elmer Ltd., Beaconsfield, UK) using λ_{exc} and λ_{em} of 380 nm and 480 nm, respectively and slits fixed at 5 nm. The fraction of bound ANS was calculated using Eq. (1):

$$[\mathrm{ANS}]_b = \frac{F_b - F_0}{A_b - A_0} \tag{1}$$

where F_b and F_0 are the fluorescence intensities of ANS with and without lipid in the cuvette and A_b and A_0 are the emission coefficients of ANS in presence and absence of lipid, respectively. Emission coefficients in presence of lipid were determined as the slope in the graphic representation of the fluorescence emission intensity at high lipid concentration (1–2 mM) as a function of low ANS concentration (0.1–1 μM) [33]. Concentration of bound ANS ($[ANS]_b$) as a function of the concentration of the free ANS ($[ANS]_{free}$) was adjusted to a Langmuir isotherm Eq. (2):

$$[\mathrm{ANS}]_b = C_{\max}\frac{(K\cdot[\mathrm{ANS}]_{\mathrm{Free}})^b}{1+(K\cdot[\mathrm{ANS}]_{\mathrm{Free}})^b} \tag{2}$$

where C_{max} is the maximum concentration of ANS bound to lipids, *K is* the binding constant and *b* is a parameter that gives information of the cooperativity of the process.

The variation of the surface potential in the membranes caused by drug incorporation was determined using the values of the different *K* obtained from Eq. (2) and introducing them in Eq. (3).

$$\Delta\Psi = \frac{RT}{F}\ln\left(\frac{K}{K_0}\right) \tag{3}$$

where *R*, *T* and *F* are the universal constant of gases, the temperature and the Faraday constant, respectively; *K and* K_0 are the apparent association constants obtained in the samples with and without drugs, respectively [34,35].

2.7. Laurdan generalized polarization studies

The effect of drugs on the gel-liquid crystalline phases of the phospholipids at the level of glycerol backbone was determined by monitoring the temperature dependence of Laurdan excitation generalized polarization. Laurdan is a polarity sensitive probe [36], located at the glycerol backbone of the bilayer with the lauric acid tail anchored in the phospholipid acyl chain region [37]. We monitored the bilayer fluidity-dependent fluorescence spectral shift of Laurdan due to dipolar relaxation phenomena. Upon excitation, the dipole moment of Laurdan increases noticeably and water molecules in the vicinity of the probe reorient around this new dipole. When the membrane is in a fluid phase, the reorientation rate is faster than the emission process and, consequently, a red-shift is observed in the emission spectrum of Laurdan. When the bilayer packing increases part of the water molecules is excluded from the bilayer and the dipolar relaxation of the remaining water molecules is slower, leading to a fluorescent spectrum which is significantly less shifted to the red [38].

Fluorescence determinations were carried out using a thermostated Perkin-Elmer LS55 fluorescence spectrophotometer at an excitation wavelength of 340 nm. The lipid concentration of liposomes was adjusted to 100 μM with 10 mM Tris–HCl, pH 7.4 and Laurdan was added from a 5×10^{-3} M stock solution of DMF to give a lipid:probe ratio of 300. Drugs were added to liposomes to a final concentration of 60 nM and incubated under continuous agitation at 37 °C out of light for 60 min. Generalized polarization (GP) from emission spectra was calculated using Eq. (4):

$$\mathrm{GP}_{ex} = \frac{I_{440} - I_{490}}{I_{440} + I_{490}} \tag{4}$$

where I_{440} and I_{490} are the fluorescence intensities at emission wavelengths of 440 nm (gel phase) and 490 nm (liquid crystalline phase), respectively, at a fixed excitation wavelength of 340 nm.

GP_{ex} values as a function of temperature were adjusted to a Boltzmann Eq. (5):

$$\mathrm{GP}_{ex} = \mathrm{GP}^2_{ex} + \frac{\mathrm{GP}^1_{ex} - \mathrm{GP}^2_{ex}}{1+\exp\left\{\frac{T_m - T}{m}\right\}} \tag{5}$$

where GP^1_{ex} and GP^2_{ex} are the maximum and minimum values of GP_{ex}, T_m the melting temperature of the composition studied and *m* is the slope of the transition that gives information of the cooperativity of the process.

2.8. DPH fluorescence polarization studies

The influence of drugs on the phase behavior of the hydrocarbon domain of the bilayer was followed by monitoring the dependence of the degree of DPH polarization degree over temperature. DPH is thought to reside in the hydrophobic core of the membrane [39–41]. For pure phospholipids, the characteristic shape of the plot is sinusoidal, with a plateau of high anisotropy values at temperatures below T_m, another plateau of low anisotropy values at temperature above T_m, and a sharp transition of anisotropy values in a short range of temperatures whose averaged value correspond to T_m. T_m is strongly dependent on the natural dynamic motions of the bilayer and shift of its values are indicative of changes of the ordering in domains where the probe is located. DPH was dissolved to a final concentration of 100 μM in tetrahydrofuran and incorporated to the sample with the lipids before evaporation to a molar ratio 300:1 (lipid: DPH). The total phospholipid concentration of each preparation was adjusted to a final value of 50 μM with 10 mM Tris–HCl, pH 7.4. Drugs (60 nM) were incubated for 60 min at 37 °C with liposomes in the dark. Anisotropy (r) of samples was determined as a function of the temperature. All fluorescence determinations were performed on an LS 55 fluorescence spectrophotometer using λ_{exc} and λ_{em} of 381 nm and 426 nm, respectively and slits fixed at 5 nm. r values were determined as shown in Eq. (6):

$$r = \frac{I_{VV} - G \cdot I_{VH}}{I_{VV} + 2 \cdot G \cdot I_{VH}} \tag{6}$$

were I_{VV} is the fluorescence intensity when angle between polarizers is 0 °, I_{VH} is the fluorescence intensity when angle between polarizers is 90 °, and G is an inherent factor to the fluorometer used. Data obtained were adjusted to a Boltzmann Eq. (7) as:

$$r = r_2 + \frac{r_1 - r_2}{1 + \exp\left\{\frac{T_m - T}{m}\right\}} \tag{7}$$

where r_1 and r_2 are the maximum and minimum values of anisotropy, T_m the melting temperature of the composition studied, and m the slope of the transition that gives information of the cooperativity of the process.

2.9. Statistical analysis

All statistical analyses were performed under GraphPad Prism version 4.3 for Windows (GraphPad Software, San Diego, CA) using two-way ANOVA using all data points for the comparison between plots or F-test when only T_m values were compared.

3. Results

3.1. Changes in bilayer morphology and thickness (AFM imaging)

AFM allows visualizing in real time the surface of cells or lipid membranes as they interact with external agents [42]. We have thus examined the effect of vancomycin and oritavancin on the topography of supported bilayers prepared from lipids extracted from *S. aureus* (Fig. 1). Due to the complex nature of the composition of *S. aureus* lipids (nearly 90–95% of charged phospholipids), the extension, and, consequently, the covering of the mica surface by the lipids, were different from one experiment to another. The supported bilayers, nevertheless, presented the same roughness and step height.

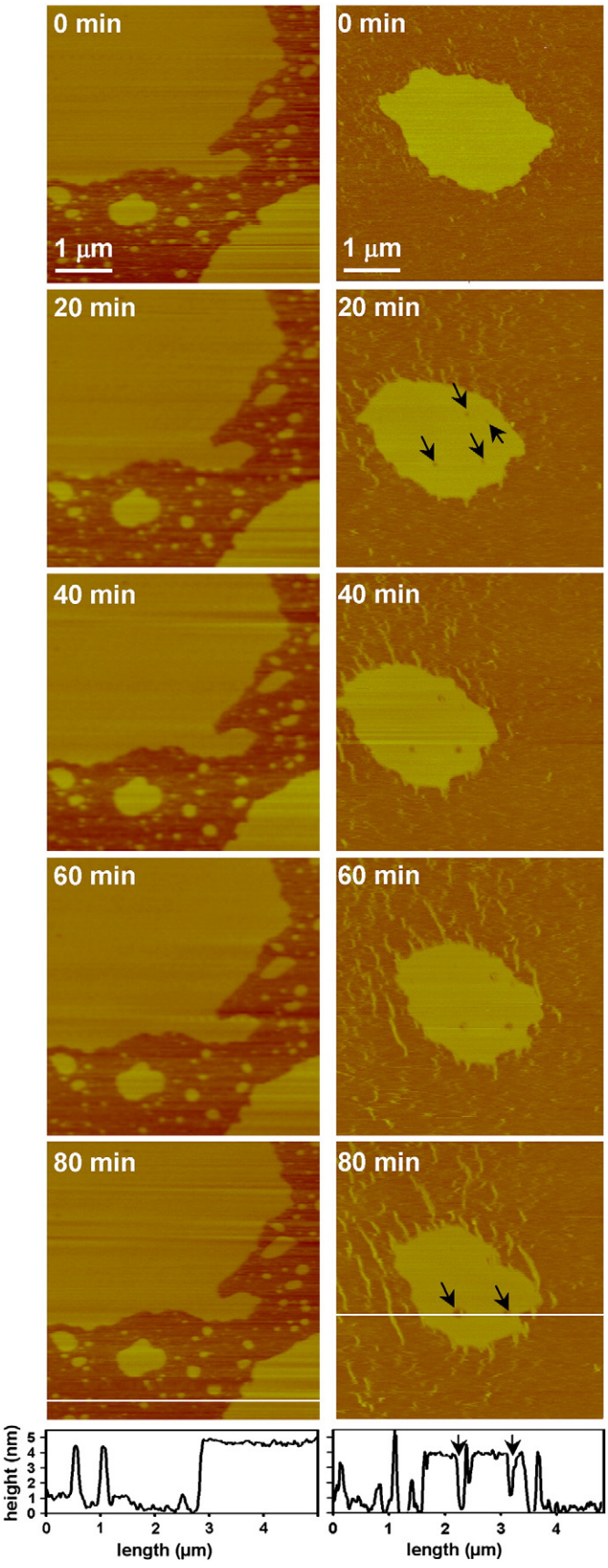

Fig. 1. Nanoscale membrane activity of vancomycin (left) or oritavancin (right) on supported bilayers prepared from lipids extracted from *S. aureus*. AFM height images (5 μm × 5 μm; z-scale: 20 nm) of supported planar bilayer recorded prior (0 min) or after exposure for 20, 40, 60 and 80 min to vancomycin (5.5 μM [8 mg/L]) (left) or oritavancin (84 nM [0.15 mg/L]) (right). Vertical cross-sections were taken along the position indicated by the continuous line (shown in the 80 min panels). Black arrows showed holes induced by oritavancin.

Vancomycin (tested at 8 mg/L [5.5 μM], corresponding to its MBC) did not induce major effect during the time of the experiment (left panels). In contrast, oritavancin (tested at 0.15 mg/L [84 nM] in 0.002% polysorbate, corresponding to MBC) induced the appearance of holes already after 20 min, and the edges of the supported bilayers were progressively eroded with time (right panels). Also, streaky features were seen in the images, presumably reflecting lipid material rearranged upon interaction with the drug. The thickness, obtained by comparing the step height in Fig. 1 between the top of the lipid layer (brightest region) to the uncovered mica (darkest region) was measured over an 80 min period after initial contact. This thickness decreased only slightly (from 5.5 ± 0.3 to 4.9 ± 0.2 nm) over the observation period when the lipid bilayers were incubated with vancomycin, but more rapidly and more markedly in the presence of oritavancin (from 5.7 ± 0.4 to 3.5 ± 0.2 nm) (Fig. 2).

3.2. Permeabilization of bilayers (release of calcein)

Since holes and decrease of the thickness appeared in the supported bilayers incubated with bactericidal concentrations of oritavancin but not with vancomycin, we compared the abilities of the two drugs to permeabilize lipid bilayers. This was assessed by following the release of calcein entrapped at self-quenching concentrations within liposomes prepared from lipids extracted from *S. aureus*. Fig. 3 shows the results obtained as a function of the drug concentration (upper panel) and of time of exposure (lower panel). Whatever its concentration (0–60 μM) and the duration of the incubation (0–24 h), vancomycin did not cause calcein release. In contrast, oritavancin, caused both a concentration- and time-dependent release of the probe. Of interest, this release became clearly detectable once the concentration had exceeded about twice the MBC of oritavancin and tended to reach a plateau at about 5- to 6-fold this concentration (upper panel). It also proceeded almost linearly with time over the first 6 h with a tendency to a plateau thereafter (lower panel).

To avoid destabilization of the bilayers, and to compare oritavancin and vancomycin at the same molar concentration, all subsequent experiments were performed at a drug concentration of 60 nM (oritavancin: 0.11 mg/L; vancomycin: 0.09 mg/L).

3.3. Binding to lipids (change in 8-anilino-1-naphthalene sulfonic acid [ANS] fluorescence)

To determine the capacity of vancomycin and oritavancin to bind to lipids extracted from *S. aureus*, we monitored the fluorescence intensity of 8-anilino-1-naphthalene sulfonic acid (ANS), a probe that binds at the membrane-water interface. Interaction between ANS and lipids induced a substantial increase in probe quantum yield. Fig. 4 shows that the fluorescence signal increased as ANS was added in increasing

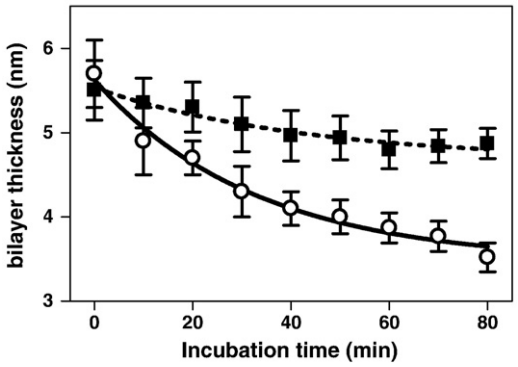

Fig. 2. Supported bilayer thickness (nm) as a function of time for lipid bilayers incubated at room temperature in buffer (20 mM Tris–HCl, 150 mM NaCl, pH 7.4) in the presence of vancomycin (squares; closed symbols; 5.5 μM [8 mg/L]) or oritavancin (circles; open symbols; 84 nM [0.15 mg/L]).

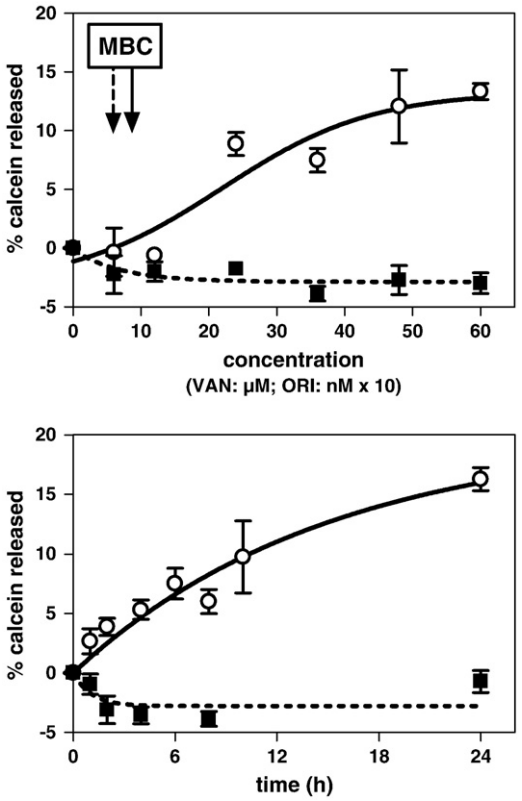

Fig. 3. Release of calcein from liposomes made of lipids extracted from *S. aureus* upon exposure at 37 °C to vancomycin (squares; closed symbols) or oritavancin (circles; open symbol). Top: effect of concentration after 8 h contact. The vertical arrows (marked MBC) point to the minimal bactericidal concentrations (3 $\log_{10}$ cfu decrease) of vancomycin (dotted line) or oritavancin (solid line) towards *S. aureus* ATCC 25923; note that the scale for vancomycin [VAN] extends from 0 to 60 μM and from 0 to 600 nM for oritavancin [ORI]). Bottom: effect of time at a fixed concentration (vancomycin: 36 μM; oritavancin: 360 nM). The ordinate shows the percentage of calcein released compared to what was observed after addition of 2% Triton X-100. Each value is the mean of 3 independent experimental determinations ± SEM.

concentrations to untreated vesicles, corresponding to the binding of the probe, until a plateau was reached at high concentrations. Fig. 4 shows also that preincubation of the vesicles with vancomycin did not markedly modify this signal, whereas it was significantly increased in vesicles preincubated with oritavancin. C_{max} (the maximum concentration of ANS bound to lipids), K (the association constant), and b (a parameter that gives information of the cooperativity of the process), were calculated after adjusting to Langmuir isotherm. With oritavancin, all the three parameters were significantly increased (C_{max}: 1.57 ± 0.05 vs. 1.26 ± 0.05; K: 55 $\mu M^{-1} \times 10^{-3}$ ± 4 vs. 43 $\mu M^{-1} \times 10^{-3}$ ± 3; b: 1.50 ± 0.16 vs. 1.25 ± 0.11). The calculated $\Delta\psi$ was + 7 ± 3 mV. With vancomycin, the C_{max} values increased (0.56 ± 0.08 vs. 0.30 ± 0.06), but no statistically significant differences were observed for K (40 ± 14 $\mu M^{-1} \times 10^{-3}$ vs. 56 ± 19 $\mu M^{-1} \times 10^{-3}$) or b (0.94 ± 0.17 vs. 0.90 ± 0.30). Moreover, no positive value of $\Delta\psi$ was observed in the presence of vancomycin.

3.4. Changes in bilayer packing and polarity at the glycerol backbone of phospholipids (generalized polarization of Laurdan)

More data regarding the physical state of the lipids can be inferred by measurement of the generalized polarization (GP_{ex}) of Laurdan. A high GP_{ex} value is usually associated with a high bilayer packing and a low polarity, whereas a low GP_{ex} value is associated with the opposite [36]. The evaluation of GP_{ex} values with temperature was shown in Fig. 5. As observed for biological membranes [43], no clear coexistence of the gel and of the liquid crystalline phase was observed. In the

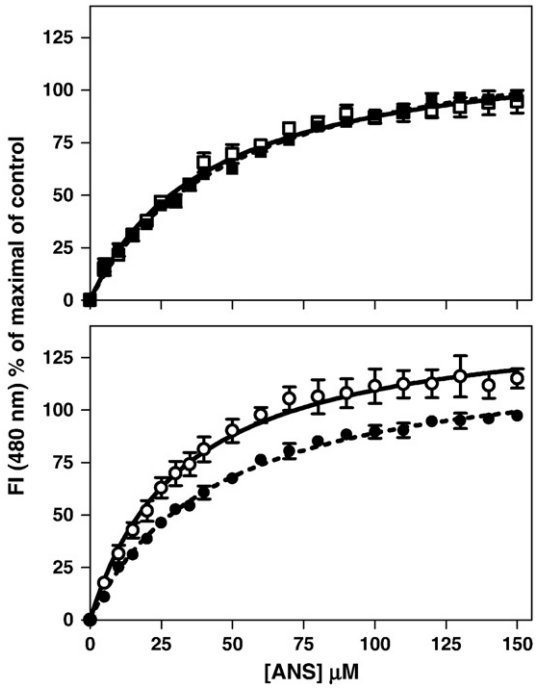

Fig. 4. Effect of vancomycin (top) and oritavancin (bottom) on ANS fluorescence as a function of free ANS. The closed and open symbols refer to data obtained in the absence or in the presence of drug, respectively. Top: ANS was added to control liposomes (closed symbols) or liposomes pre-exposed to vancomycin (60 nM; open symbols). Bottom: ANS was added to control liposomes (closed symbols) or to liposomes pre-exposed to oritavancin (60 nM; open symbols). The total lipid concentration was 50 μM. Each value is the average of three independent experiments. Statistical analysis (2-ways ANOVA comparing all data points): the p values versus control are 0.517 and <0.0001 for vancomycin and oritavancin, respectively.

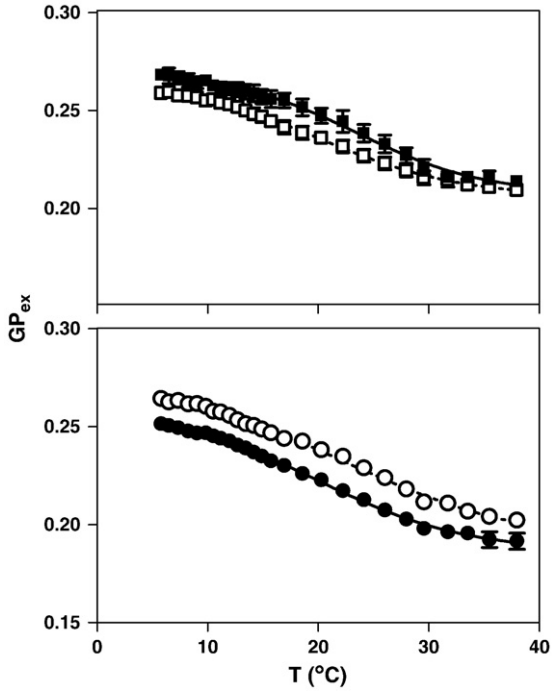

Fig. 5. Effect of vancomycin (top) and oritavancin (bottom) on generalized polarization (GP_{ex}) values for Laurdan in vesicles made of *S. aureus* lipids as a function of temperature. The closed and open symbols refer to data obtained in absence or presence of drug (60 nM), respectively. The excitation wavelength was fixed at 340 nm and emission intensities at 440 nm (gel phase) and 490 nm (liquid crystalline phase). Each value is the average of three independent experiments. Statistical analysis (2-ways ANOVA comparing all data points): the p values vs. control are <0.0001.

presence of glycopeptides, GP_{ex} values decreased as a function of temperature similarly to controls. Both vancomycin and oritavancin induced a significant effect ($p<0.0001$) dependent on the nature of the antibiotic. Vancomycin induced a shift to slightly lower values with a decrease of the T_m values from 23.6 ± 1.0 °C to 20.1 ± 0.9 °C ($p<0.02$). In contrast, oritavancin markedly shifted GP_{ex} values towards higher values with a variation of T_m from 19.9 ± 0.6 °C to 22.3 ± 0.7 °C ($p<0.02$).

3.5. Changes in the hydrophobic core of bilayers (DPH fluorescence anisotropy)

To determine the effect of vancomycin and oritavancin on the acyl chain ordering in the hydrophobic core region of the membrane of liposomes, we measured the change in fluorescence anisotropy of the hydrophobic probe DPH upon temperature increase. As shown in Fig. 6, the DPH-steady state fluorescence anisotropy intensity gradually declined as the temperature increased from 3 to 37 °C. As for GP_{ex} determinations, no sharp phase transitions were observed and a continuous decrease of depolarization intensities with increasing temperature was seen. Compared to their respective control, no gross effect of vancomycin or oritavancin was observed. However, statistical analysis showed that vancomycin induced a slight increase of the DPH-steady state fluorescence depolarization intensities upon increasing temperatures ($p<0.001$) (Fig. 6, upper panel) whereas oritavancin had the opposite effect ($p=0.0005$) (Fig. 6, lower panel). The T_m values were slightly increased with vancomycin (15.9 ± 0.4 °C vs. 19.0 ± 0.8 °C; $p<0.005$) and not significantly modified with oritavancin (12.5 ± 1.3 °C vs. 11.0 ± 2.0 °C; $p<0.02$).

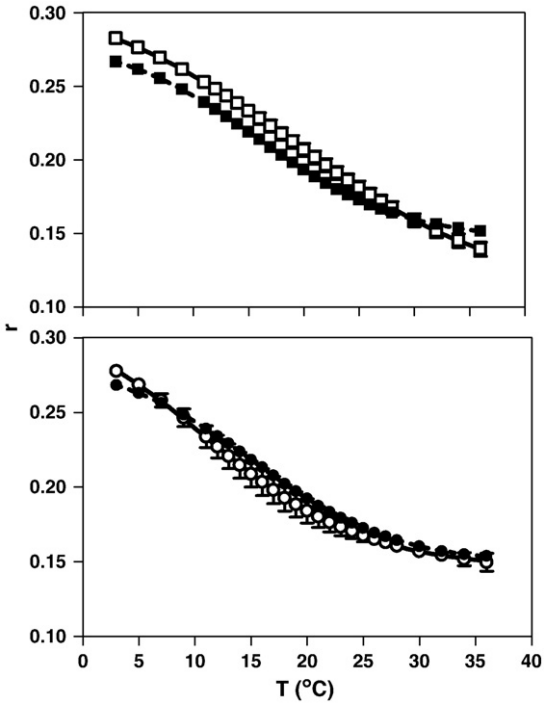

Fig. 6. Effect of vancomycin (top) and oritavancin (bottom) on fluorescence anisotropy (r) of DPH in lipid vesicles upon increasing temperatures. The closed and open symbols refer to data obtained in the absence or in the presence of drug, respectively. DPH was incorporated at a molar ratio to the lipids of 1:300. Labeled liposomes were incubated with drugs (60 nM) at 37 °C for 30 min. Liposomes were then brought to 3 °C, stabilized at this temperature during 15 min before starting the measurements, during which the samples were heated to 40 °C at a rate of 16 °C/h. Data are representative of experiments that were reproduced three times. Statistical analysis (2-ways ANOVA comparing all data points): p value vs. control: <0.0001 for vancomycin and 0.0005 for oritavancin).

3.6. Changes in GP_{ex} of Laurdan and in anisotropy of DPH on POPE:CL and LysylDOPG:POPG:POPE vesicles

To further characterize the specific role played by individual lipids on the effects of glycopeptides at the level of glycerol backbone and deeper in the bilayer, we reproduced these experiments using (LysylDOPG:POPG:POPE (0.5:8:4) and CL:POPE (2:8) liposomes. Investigating the role of cardiolipin (an anionic lipid) and lysylphosphatidylglycerol (a positively charged lipid) was of particular interest since a decrease in the net negative charge of the cell envelope is a strategy used by numerous bacteria, including *S. aureus*, to modulate their affinity for cationic antibiotic microbial molecules [44]. Moreover, we showed previously that the increase of membrane permeability induced by oritavancin is maximal in the presence of cardiolipin [23]. Thus, we examined, and show in Fig. 7, the effect of oritavancin on Laurdan generalized polarization (left panel) and anisotropy fluorescence of DPH (right panel) on CL:POPE (2:8) (top) and on LysylDOPG:POPG:POPE (0.5:8:4) (bottom) vesicles.

First, in contrast to what was observed with lipids extracted from *S. aureus*, and as largely reported in literature, the thermotropic behavior of synthetic and/or defined lipids clearly showed the appearance of gel and liquid phases with a defined T_m. This is well illustrated for LysylDOPG:POPG:POPE (Fig. 7, lower panels). In the presence of cardiolipin, a natural lipid for which the length and the degree of unsaturation are not defined, the phase separation was less marked, probably due to the variability of the length as well as the degree of insaturation of the acyl chains of cardiolipin. Second, when oritavancin was added to CL:POPE liposomes, we confirmed its ability to induce an increase of GP_{ex} values, especially at temperatures around the T_m with an increase from 13.5 ± 1.7 to 15.5 ± 1.1 ($p < 0.001$). No effect was observed at low and high temperatures. In contrast, when oritavancin was added to LysylDOPG:POPG:POPE liposomes, a slight decrease of GP_{ex} values was observed with a decrease of T_m from 23.0 ± 0.4 to 21.2 ± 0.3 ($p < 0.001$). As observed with vesicles made of lipids extracted from *S. aureus*, oritavancin very slightly affected the fluorescence polarization values of DPH.

4. Discussion

The present study expands over our previous observations concerning the ability of oritavancin, a novel lipoglycopeptide antibiotic with marked bactericidal activity against *S. aureus* and other Gram-positive bacteria, to destabilize model membrane bilayers (liposomes) when these contain a large proportion of acidic phospholipids such as phosphatidylglycerol and cardiolipin [23]. The present study aimed at gaining additional insight into the molecular mechanism of this phenomenon by (i) using lipids extracted from the target bacteria themselves; (ii) examining the influence exerted by oritavancin at the levels of glycerol backbone and the hydrophobic core of the bilayers; (iii) systematically comparing oritavancin with the prototype glycopeptides antibiotic vancomycin at concentrations that are close to those at which these drugs exert a bactericidal effect towards *S. aureus* in conventional microbiological studies.

AFM provides a true three-dimensional map of the surface of the samples at a submicron scale together with the capacity to analyze them as immersed in defined fluids [42]. Our observations provide direct evidence for the ability of oritavancin, but not of vancomycin, to induce holes in membranes, which is confirmed by the results of the calcein release experiments. The mechanisms responsible for membrane permeabilization are complex but three main ones have been proposed (see [45] for review). The first is related to the presence of local microscopic regions of disorder or defects enhanced by drugs. The enhancement of permeability would, therefore, be due to instability of boundary regions around the interdigitated structure domains, characterized by a thinner structure and more rigid hydrocarbon regions than its non-interdigitated counterpart. The two other mechanisms involved in membrane permeabilization are the partitioning of the drug monomer into the lipid bilayer and oligomerization as well as the

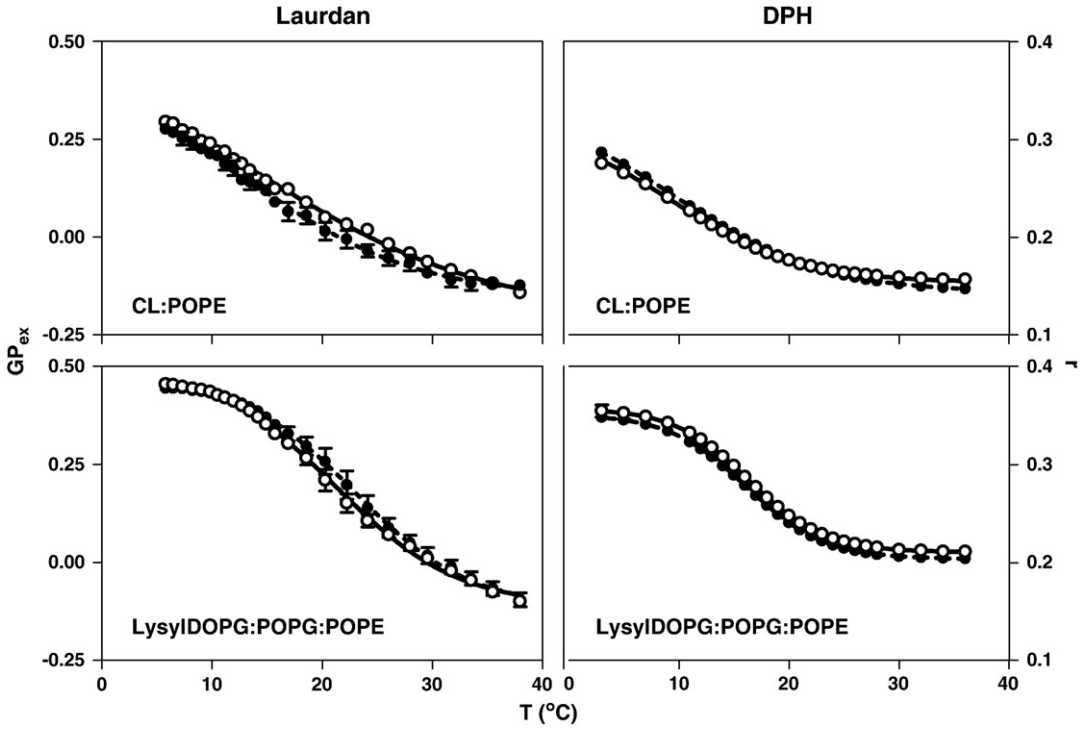

Fig. 7. Effect of oritavancin (60 nM) on generalized polarization values (GP_{ex}) for Laurdan (left) or fluorescence anisotropy polarization (r) for DPH (right) in phospholipid vesicles of CL:POPE (top) and lysylDOPG:POPG:POPE (bottom) upon increasing temperatures. Statistical analysis (2-ways ANOVA comparing all data points): all p values vs. controls are < 0.0001 except for oritavancin in Laurdan assay with LysylDOPG:POPG:POPE ($p < 0.0114$) and DPH experiment with CL:POPE ($p < 0.0740$).

imbalance between the inner and the outer monolayer resulting from the binding of the drug to the outer membrane. The latter feature is a key parameter for driving shape changes and curvature stress. AFM could not directly visualize oritavancin binding. In future work, it would be interesting to examine whether friction images could reveal any contrast associated with oritavancin binding.

In the present work, we characterize the molecular interactions between oritavancin and lipids, using fluorescence approaches to determine in one hand the ability of oritavancin to bind to lipid membranes mimicking the bilayer of *S. aureus*, and, in the other hand, to know at which level oritavancin most likely interacts in the bilayer (glycerol backbone vs. hydrocarbon chains). This was made by using ANS, Laurdan and DPH. ANS is a negatively charged dye with a higher fluorescence yield in lipid than in aqueous environments. Being repulsed by the membrane, an increase in its binding must be interpreted as a decrease of the global negative charges of the surface of the bilayer. This property has been used to characterize the interaction of drugs [34,46], bactericidal peptides [47], or cytochrome c [48,49] with lipids, and to study intracellular lipid-binding proteins [50]. Laurdan, which localizes at ~11.4 Å from the bilayer center [51], shows fluorescence excitation and emission spectra that are affected by the lipid packing, the rate of dipolar relaxation and the hydrophilic/hydrophobic character of its surrounding environment [36,38,43,52]. It has been successfully used to study the interactions of peptides [53,54], including toxins [55,56] or proteins [57], with lipid bilayers. DPH is a an hydrophobic probe widely used for testing the fluidity of the inner core of the bilayer [39–41]. Interpreting our data with oritavancin, in comparison with vancomycin, must take into account that oritavancin is both more cationic (due to the presence of an epivancosamine moiety absent in vancomycin), and more hydrophobic (with calculated log *P* and log D_{pH7} of 4.10 and −3.43 vs. −1.44 and −4.70 for vancomycin). We see that oritavancin (i) markedly increases the binding of ANS and modifies the interactions of Laurdan with the adjacent water molecules, while having only a very modest effect on the fluorescence polarization of DPH. Vancomycin had only limited effects with respect to ANS and Laurdan, and its influence on the fluorescence polarization of DPH is also quite modest and in the opposite direction to that of oritavancin. Together, these experiments strongly suggest that oritavancin binds to the bilayers (thereby reducing its negative surface charge) and interacts at the level of the glycerol backbone by hindering the accessibility of water and rigidifying the lipid bilayer. Oritavancin, however, would not markedly affect the deeper domains of the bilayer. Vancomycin is without major effect on either domain of the bilayer, due to its lack of binding under the *in vitro* conditions used here. Thus, ordering at the level of glycerol backbone, which is the first of the mechanisms discussed above [45], could be critical for subsequent lipid permeabilization. This conclusion is consistent with our previous studies with model POPG:POPE bilayer membranes that showed a high propensity of oritavancin to interact through hydrogen bonds with phosphate and carbonyl oxygen atoms as well as a much denser packing of chain atoms in the near surface regions of the hydrocarbon core [23].

The membranes prepared here were made of a mixture of lipids extracted from *S. aureus*. The major lipids present are phosphatidylglycerol, cardiolipin and lysylphosphatidylglycerol, a lipid synthesized by the membrane protein MprF [58,59]. These differ by their structure, charge, non-lamellar propensity and cross-sectional area. These lipids can also exist in a variety of organized supramolecular structures and interact dynamically to form transient arrangements. The use of natural lipid extracts explains the lack of sharp transition between the gel and liquid crystal phase compared to what is seen liposomes made of synthetic lipids. Similarly, the cohesive effect of oritavancin on GP_{ex} was smaller on vesicles prepared from lipid extracts as compared to those composed of CL:POPE, and the calcein release was less important [23]. Differences in membrane permeability properties have already been observed when comparing vesicles made of lipids extracted from bacteria to those made of pure lipids or binary mixtures of phospholipids [60]. Further experiments will need to examine the reasons for these differences. For vesicles made of LysylDOPG:POPG:POPE, the decrease of the negative charge of the membrane probably explains the absence of major effect of oritavancin on GP_{ex} and fluorescence anisotropy values. Accordingly, *S. aureus mprF* mutants show a decreased susceptibility to cationic antimicrobial peptides of the innate immune system and vancomycin [61] and to the membrane permeabilizing antibiotic daptomycin [62].

Together, our data confirm the interactions of oritavancin with *S. aureus* membrane lipids and its capacity to permeabilize lipid vesicles made of these lipids at concentrations at which the drug is known to exert a bactericidal effect on bacteria. It is, therefore, tempting to speculate that this may be the basis of its marked and fast bactericidal effect [63], including against non-growing bacteria [15], making it quite distinct from vancomycin in this context. As discussed previously [23], the specificity of oritavancin action towards bacteria vs. eukaryotic cells, probably stems from (i) the presence of free D-Ala-D-Ala motifs at the inner face of the cell wall (peptidoglycan) that allows an anchoring the drug close to the bacterial membrane (see model in [1]) and (ii) the abundance in *S. aureus* of negatively charged lipids (phosphatidylglycerol and cardiolipin) that are critical for interaction of the drug with the bilayer but are rare in the eukaryotic pericellular membrane. Such differences in drug–lipid membrane interactions have also been reported for a hydrophobic membrane-binding peptide antibiotic, NK2, that regulates the structure of the membrane and kills bacterial but not human cells [64] or for cecropin-melittin antimicrobial hybrid peptide BP100 [65]. The present data do not exclude that other mechanisms, such as inhibition of transglycosylase activity [66] or additional binding with cell wall pentaglycyl bridges [67,68], could also contribute to the antibacterial effects of oritavancin. However, none of them explains as such the intense bactericidal activity of oritavancin at the low concentrations at which it can be observed.

In conclusion, we have provided here a comprehensive study of the interaction of oritavancin, a novel lipoglycopeptide endowed with potent antimicrobial activity, with phospholipid bilayers prepared with lipids extracted from *S. aureus*. We elucidated fundamental issues such as the specific interaction of oritavancin at the level of the glycerol backbone and the hydrophobic domain of the bilayer by monitoring Laurdan excitation GP_{ex} and fluorescence anisotropy of DPH, respectively. Oritavancin induces higher GP_{ex} values and increase of transition temperature indicating a membrane in a more ordered structure at the level of the glycerol backbone of the lipid bilayer where Laurdan is localized. In the non-polar environment where DPH incorporates, oritavancin slightly decreases the fluorescence depolarization intensities, suggesting a modest increase in fluidity. Altogether, these effects could be related to the ability of oritavancin antibiotic to induce holes, erosion of the edges and decrease of the thickness of the supported lipid bilayers as well as to increase membrane permeabilization. Progress in understanding the lipid–drug interactions appears to be of crucial importance to understand the mechanisms involved in antibacterial activity of new compounds.

Acknowledgments

Y.D. and F.V. B. are Senior Research Associates of the Belgian Fonds de la Recherche Scientifique (F.R.S.-FNRS). This work was supported by the Région wallonne (NANOMEMB), the F.R.S.-FNRS (grant no. 1.5.236.08 F), the Fonds de la Recherche Scientifique Médicale (FRSM grants no. 3.4.588.10F and FRFC grants no. 3.4.566.09F), the Université catholique de Louvain (Fonds Spéciaux de Recherche and Actions de Recherche Concertées), and with a grant-in-aid from Targanta Therapeutics (a wholly owned subsidiary of The Medicines Company).

References

[1] F. Van Bambeke, M.P. Mingeot-Leclercq, M.J. Struelens, P.M. Tulkens, The bacterial envelope as a target for novel anti-MRSA antibiotics, Trends Pharmacol. Sci. 29 (2008) 124–134.

[2] A.Z. Sahalan, R.A. Dixon, Role of the cell envelope in the antibacterial activities of polymyxin B and polymyxin B nonapeptide against Escherichia coli, Int. J. Antimicrob. Agents 31 (2008) 224–227.

[3] C. Toniolo, M. Crisma, F. Formaggio, C. Peggion, R.F. Epand, R.M. Epand, Lipopeptaibols, a novel family of membrane active, antimicrobial peptides, Cell. Mol. Life Sci. 58 (2001) 1179–1188.

[4] S. Oancea, G. Hilma, C. Peggion, F. Formaggio, C. Toniolo, Main-chain length control of conformation, membrane activity, and antibiotic properties of lipopeptaibol sequential analogues, Chem. Biodivers. 5 (2008) 681–692.

[5] P. Mak, J. Pohl, A. Dubin, M.S. Reed, S.E. Bowers, M.T. Fallon, W.M. Shafer, The increased bactericidal activity of a fatty acid-modified synthetic antimicrobial peptide of human cathepsin G correlates with its enhanced capacity to interact with model membranes, Int. J. Antimicrob. Agents 21 (2003) 13–19.

[6] H. Wakabayashi, H. Matsumoto, K. Hashimoto, S. Teraguchi, M. Takase, H. Hayasawa, N-Acylated and D enantiomer derivatives of a nonamer core peptide of lactoferricin B showing improved antimicrobial activity, Antimicrob. Agents Chemother. 43 (1999) 1267–1269.

[7] A. Majerle, J. Kidric, R. Jerala, Enhancement of antibacterial and lipopolysaccharide binding activities of a human lactoferrin peptide fragment by the addition of acyl chain, J. Antimicrob. Chemother. 51 (2003) 1159–1165.

[8] D. Avrahami, Y. Shai, Bestowing antifungal and antibacterial activities by lipophilic acid conjugation to D,L-amino acid-containing antimicrobial peptides: a plausible mode of action, Biochemistry 42 (2003) 14946–14956.

[9] C. Chicharro, C. Granata, R. Lozano, D. Andreu, L. Rivas, N-terminal fatty acid substitution increases the leishmanicidal activity of CA(1-7)M(2-9), a cecropin-melittin hybrid peptide, Antimicrob. Agents Chemother. 45 (2001) 2441–2449.

[10] S. Bera, G.G. Zhanel, F. Schweizer, Design, synthesis, and antibacterial activities of neomycin-lipid conjugates: polycationic lipids with potent gram-positive activity, J. Med. Chem. 51 (2008) 6160–6164.

[11] I. Baussanne, A. Bussiere, S. Halder, C. Ganem-Elbaz, M. Ouberai, M. Riou, J.M. Paris, E. Ennifar, M.P. Mingeot-Leclercq, J.L. Decout, Synthesis and antimicrobial evaluation of amphiphilic neamine derivatives, J. Med. Chem. 53 (2010) 119–127.

[12] R.D. Cooper, N.J. Snyder, M.J. Zweifel, M.A. Staszak, S.C. Wilkie, T.I. Nicas, D.L. Mullen, T.F. Butler, M.J. Rodriguez, B.E. Huff, R.C. Thompson, Reductive alkylation of glycopeptide antibiotics: synthesis and antibacterial activity, J. Antibiot. Tokyo 49 (1996) 575–581.

[13] M.R. Leadbetter, S.M. Adams, B. Bazzini, P.R. Fatheree, D.E. Karr, K.M. Krause, B.M. Lam, M.S. Linsell, M.B. Nodwell, J.L. Pace, K. Quast, J.P. Shaw, E. Soriano, S.G. Trapp, J.D. Villena, T.X. Wu, B.G. Christensen, J.K. Judice, Hydrophobic vancomycin derivatives with improved ADME properties: discovery of telavancin (TD-6424), J. Antibiot. Tokyo 57 (2004) 326–336.

[14] D.L. Higgins, R. Chang, D.V. Debabov, J. Leung, T. Wu, K.M. Krause, E. Sandvik, J.M. Hubbard, K. Kaniga, D.E. Schmidt, Q. Gao, R.T. Cass, D.E. Karr, B.M. Benton, P.P. Humphrey, Telavancin, a multifunctional lipoglycopeptide, disrupts both cell wall synthesis and cell membrane integrity in methicillin-resistant *Staphylococcus aureus*, Antimicrob. Agents Chemother. 49 (2005) 1127–1134.

[15] A. Belley, E. Neesham-Grenon, G. McKay, F.F. ArhinF, R. Harris, T. Beveridge, T.R. Parr, G. Moeck, Oritavancin kills stationary-phase and biofilm *Staphylococcus aureus* cells in vitro, Antimicrob. Agents Chemother. 53 (2009) 918–925.

[16] P.K. Linden, Vancomycin resistance: are there better glycopeptides coming? Expert Rev. Anti Infect. Ther. 6 (2008) 917–928.

[17] G.A. McKay, S. Beaulieu, F.F. Arhin, A. Belley, I. Sarmiento, T. Parr Jr., G. Moeck, Time-kill kinetics of oritavancin and comparator agents against *Staphylococcus aureus*, *Enterococcus faecalis* and *Enterococcus faecium*, J. Antimicrob. Chemother. 63 (2009) 1191–1199.

[18] M. Arthur, P.E. Reynolds, F. Depardieu, S. Evers, S. Dutka-Malen, R. Quintiliani Jr., P. Courvalin, P, Mechanisms of glycopeptide resistance in enterococci, J. Infect. 32 (1996) 11–16.

[19] P.E. Reynolds, Structure, biochemistry and mechanism of action of glycopeptide antibiotics, Eur. J. Clin. Microbiol. Infect. Dis. 8 (1989) 943–950.

[20] R.C. Mercier, C. Stumpo, M.J. Rybak, Effect of growth phase and pH on the in vitro activity of a new glycopeptide, oritavancin (LY333328), against *Staphylococcus aureus* and Enterococcus faecium, J. Antimicrob. Chemother. 50 (2002) 19–24.

[21] E. Tuomanen, Phenotypic tolerance: the search for beta-lactam antibiotics that kill nongrowing bacteria, Rev. Infect. Dis. 8 (Suppl 3) (1986) S279–S291.

[22] M.M. Lleo, D. Benedetti, M.C. Tafi, C. Signoretto, P. Canepari, Inhibition of the resuscitation from the viable but non-culturable state in *Enterococcus faecalis*, Environ. Microbiol. 9 (2007) 2313–2320.

[23] O. Domenech, G. Francius, P.M. Tulkens, F. Van Bambeke, Y. Dufrene, M.P. Mingeot-Leclercq, Interactions of oritavancin, a new lipoglycopeptide derived from vancomycin, with phospholipid bilayers: effect on membrane permeability and nanoscale lipid membrane organization, Biochim. Biophys. Acta 1788 (2009) 1832–1840.

[24] A.M. Seddon, D. Casey, R.V. Law, A. Gee, R.H. Templer, O. Ces, Drug interactions with lipid membranes, Chem. Soc. Rev. 38 (2009) 2509–2519.

[25] C. Peetla, A. Stine, V. Labhasetwar, Biophysical interactions with model lipid membranes: applications in drug discovery and drug delivery, Mol. Pharm. 6 (2009) 1264–1276.

[26] F. Van Bambeke, M.P. Mingeot-Leclercq, A. Schanck, R. Brasseur, P.M. Tulkens, Alterations in membrane permeability induced by aminoglycoside antibiotics: studies on liposomes and cultured cells, Eur. J. Pharmacol. 247 (1993) 155–168.

[27] Clinical and Laboratory Standards Institute, Performance standards for antimicrobial susceptibility testing; 18th informational supplement, Clinical and Laboratory Standards Institute), p. approved standard M100-S18, Clinical and Laboratory Standards Institute, Wayne, Pennsylvania, 2008.

[28] F.F. Arhin, I. Sarmiento, A. Belley, G.A. McKay, D.C. Draghi, P. Grover, D.F. Sahm, T.R. Parr Jr., G. Moeck, Effect of polysorbate-80 on oritavancin binding to plastic surfaces—implications for susceptibility testing, Antimicrob. Agents Chemother. 52 (2008) 1597–1603.

[29] F.F. Arhin, D.C. Draghi, C.M. Pillar, T.R. Parr Jr., G. Moeck, D.F. Sahm, Comparative in vitro activity profile of oritavancin against recent Gram-positive clinical isolates, Antimicrob. Agents Chemother. 53 (2009) 4762–4771.

[30] F.F. Arhin, I. Sarmiento, T.R. Parr Jr., G. Moeck, Comparative in vitro activity of oritavancin against *Staphylococcus aureus* strains that are resistant, intermediate or heteroresistant to vancomycin, J. Antimicrob. Chemother. 64 (2009) 868–870.

[31] G.R. Bartlett, Colorimetric assay methods for free and phosphorylated glyceric acids, J. Biol. Chem. 234 (1959) 469–471.

[32] J.N. Weinstein, S. Yoshikami, P. Henkart, R. Blumenthal, W.A. Hagins, Liposome-cell interaction: transfer and intracellular release of a trapped fluorescent marker, Science 195 (1977) 489–492.

[33] J.Y. Ma, J.K. Ma, K.C. Weber, Fluorescence studies of the binding of amphiphilic amines with phospholipids, J. Lipid Res. 26 (1985) 735–744.

[34] M.T. Montero, M. Pijoan, S. Merino-Montero, T. Vinuesa, J. Hernandez-Borrell, Interfacial membrane effects of fluoroquinolones as revealed by a combination of fluorescence binding experiments and atomic force microscopy observations, Langmuir 22 (2006) 7574–7578.

[35] M. Sugawara, A. Hashimoto, M. Kobayashi, K. Iseki, K. Miyazaki, Effect of membrane surface potential on the uptake of anionic compounds by liposomes, Biochim. Biophys. Acta 1192 (1994) 241–246.

[36] T. Parasassi, G. De Stasio, G. Ravagnan, R.M. Rusch, E. Gratton, Quantitation of lipid phases in phospholipid vesicles by the generalized polarization of Laurdan fluorescence, Biophys. J. 60 (1991) 179–189.

[37] P.L. Chong, P.T. Wong, Interactions of Laurdan with phosphatidylcholine liposomes: a high pressure FTIR study, Biochim. Biophys. Acta 1149 (1993) 260–266.

[38] T. Parasassi, G. De Stasio, A. d'Ubaldo, E. Gratton, Phase fluctuation in phospholipid membranes revealed by Laurdan fluorescence, Biophys. J. 57 (1990) 1179–1186.

[39] M. Shinitzky, Y. Barenholz, Fluidity parameters of lipid regions determined by fluorescence polarization, Biochim. Biophys. Acta 515 (1978) 367–394.

[40] B.R. Lentz, Use of fluorescent probes to monitor molecular order and motions within liposome bilayers, Chem. Phys. Lipids 64 (1993) 99–116.

[41] R.D. Kaiser, E. London, Location of diphenylhexatriene (DPH) and its derivatives within membranes: comparison of different fluorescence quenching analyses of membrane depth, Biochemistry 37 (1998) 8180–8190.

[42] M.P. Mingeot-Leclercq, M. Deleu, R. Brasseur, Y.F. Dufrene, Atomic force microscopy of supported lipid bilayers, Nat. Protoc. 3 (2008) 1654–1659.

[43] T. Parasassi, M. Loiero, M. Raimondi, G. Ravagnan, E. Gratton, Absence of lipid gel-phase domains in seven mammalian cell lines and in four primary cell types, Biochim. Biophys. Acta 1153 (1993) 143–154.

[44] K. Mukhopadhyay, W. Whitmire, Y.Q. Xiong, J. Molden, T. Jones, A. Peschel, P. Staubitz, J. Adler-Moore, P.J. McNamara, R.A. Proctor, M.R. Yeaman, A.S. Bayer, In vitro susceptibility of *Staphylococcus aureus* to thrombin-induced platelet microbicidal protein-1 (tPMP-1) is influenced by cell membrane phospholipid composition and asymmetry, Microbiology 153 (2007) 1187–1197.

[45] K. Lohner, S.E. Blondelle, Molecular mechanisms of membrane perturbation by antimicrobial peptides and the use of biophysical studies in the design of novel peptide antibiotics, Comb. Chem. High Throughput Screen. 8 (2005) 241–256.

[46] J.L. Vazquez, M. Berlanga, S. Merino, O. Domenech, M. Vinas, M.T. Montero, J. Hernandez-Borrell, Determination by fluorimetric titration of the ionization constants of ciprofloxacin in solution and in the presence of liposomes, Photochem. Photobiol. 73 (2001) 14–19.

[47] A. Ramamoorthy, S. Thennarasu, A. Tan, D.K. Lee, C. Clayberger, A.M. Krensky, Cell selectivity correlates with membrane-specific interactions: a case study on the antimicrobial peptide G15 derived from granulysin, Biochim. Biophys. Acta 1758 (2006) 154–163.

[48] J. Teissie, A. Baudras, A fluorescence study of the binding of cytochrome C to mixed-phospholipid microvesicles : evidence for a preferred orientation of the bound protein, Biochimie 59 (1977) 693–703.

[49] O. Domenech, L. Redondo, M.T. Montero, J. Hernandez-Borrell, Specific adsorption of cytochrome C on cardiolipin-glycerophospholipid monolayers and bilayers, Langmuir 23 (2007) 5651–5656.

[50] C.D. Kane, D.A. Bernlohr, A simple assay for intracellular lipid-binding proteins using displacement of 1-anilinonaphthalene 8-sulfonic acid, Anal. Biochem. 233 (1996) 197–204.

[51] P. Jurkiewicz, A. Olzynska, M. Langner, M. Hof, Headgroup hydration and mobility of DOTAP/DOPC bilayers: a fluorescence solvent relaxation study, Langmuir 22 (2006) 8741–8749.

[52] J. Sykora, M. Hof, Solvent relaxation in phospholipid bilayers: physical understanding and biophysical applications, Cell. Mol. Biol. Lett. 7 (2002) 259–261.

[53] J.J. Kremer, D.J. Sklansky, R.M. Murphy, Profile of changes in lipid bilayer structure caused by beta-amyloid peptide, Biochemistry 40 (2001) 8563–8571.

[54] R. Esquembre, J.A. Poveda, C.R. Mateo, Biophysical and functional characterization of an ion channel peptide confined in a sol-gel matrix, J. Phys. Chem. B 113 (2009) 7534–7540.

[55] W. Huang, L.P. Vernon, L.D. Hansen, J.D. Bell, Interactions of thionin from Pyrularia pubera with dipalmitoylphosphatidylglycerol large unilamellar vesicles, Biochemistry 36 (1997) 2860–2866.
[56] M.R. Gonzalez-Baro, H. Garda, R. Pollero, Effect of fenitrothion on dipalmitoyl and 1-palmitoyl-2-oleoylphosphatidylcholine bilayers, Biochim. Biophys. Acta 1468 (2000) 304–310.
[57] T. Granjon, M.J. Vacheron, C. Vial, R. Buchet, Mitochondrial creatine kinase binding to phospholipids decreases fluidity of membranes and promotes new lipid-induced beta structures as monitored by red edge excitation shift, laurdan fluorescence, and FTIR, Biochemistry 40 (2001) 6016–6026.
[58] D.C. White, F.E. Frerman, Extraction, characterization, and cellular localization of the lipids of *Staphylococcus aureus*, J. Bacteriol. 94 (1967) 1854–1867.
[59] H. Roy, M. Ibba, Monitoring Lys-tRNA(Lys) phosphatidylglycerol transferase activity, Methods 44 (2008) 164–169.
[60] M.L. Fernandez Murga, D. Bernik, V. Font, A.E. Disalvo, Permeability and stability properties of membranes formed by lipids extracted from Lactobacillus acidophilus grown at different temperatures, Arch. Biochem. Biophys. 364 (1999) 115–121.
[61] A. Ruzin, A. Severin, S.L. Moghazeh, J. Etienne, P.A. Bradford, S.J. Projan, D.M. Shlaes, Inactivation of mprF affects vancomycin susceptibility in *Staphylococcus aureus*, Biochim. Biophys. Acta 1621 (2003) 117–121.
[62] L. Friedman, J.D. Alder, J.A. Silverman, Genetic changes that correlate with reduced susceptibility to daptomycin in *Staphylococcus aureus*, Antimicrob. Agents Chemother. 50 (2006) 2137–2145.
[63] T.I. Nicas, D.L. Mullen, J.E. Flokowitsch, D.A. Preston, N.J. Snyder, M.J. Zweifel, S.C. Wilkie, M.J. Rodriguez, R.C. Thompson, R.D. Cooper, Semisynthetic glycopeptide antibiotics derived from LY264826 active against vancomycin-resistant enterococci, Antimicrob. Agents Chemother. 40 (1996) 2194–2199.
[64] R. Willumeit, M. Kumpugdee, S.S. Funari, K. Lohner, B.P. Navas, K. Brandenburg, S. Linser, J. Andra, Structural rearrangement of model membranes by the peptide antibiotic NK-2, Biochim. Biophys. Acta 1669 (2005) 125–134.
[65] R. Ferre, M.N. Melo, A.D. Correia, L. Feliu, E. Bardaji, M. Planas, M. Castanho, Synergistic effects of the membrane actions of cecropin-melittin antimicrobial hybrid peptide BP100, Biophys. J. 96 (2009) 1815–1827.
[66] N.E. Allen, T.I. Nicas, Mechanism of action of oritavancin and related glycopeptide antibiotics, FEMS Microbiol. Rev. 26 (2003) 511–532.
[67] S.J. Kim, L. Cegelski, D. Stueber, M. Singh, E. Dietrich, K.S. Tanaka, T.R. Parr Jr., A.R. Far, J. Schaefer, Oritavancin exhibits dual mode of action to inhibit cell-wall biosynthesis in *Staphylococcus aureus*, J. Mol. Biol. 377 (2008) 281–293.
[68] G.J. Patti, S.J. Kim, T.Y. Yu, E. Dietrich, K.S. Tanaka, T.R. Parr Jr., A.R. Far, J. Schaefer, Vancomycin and oritavancin have different modes of action in Enterococcus faecium, J. Mol. Biol. 392 (2009) 1178–1191.